Gluon Fragmentation to $^1D_2$ Quarkonia

Peter Cho[1] and Mark B. Wise[2]

Lauritsen Laboratory

California Institute of Technology

Pasadena, CA 91125

Abstract

Gluon fragmentation to heavy $J^{PC} = 2^{-+}$ quarkonia is studied herein. We compute these D-wave states' polarized fragmentation functions and find that they are enhanced by large numerical prefactors. The prospects for detecting the lowest lying $^1D_2$ charmonium state at the Tevatron are discussed.

10/94

One of the outstanding challenges in QCD is to understand the process whereby colored quarks and gluons hadronize into colorless mesons and baryons. Until recently, the only basis for parton fragmentation intuition came from simple models and empirical observations. However within the past two years, important progress has been made in understanding hadronization from first principles [1–5]. It is now possible to calculate the fragmentation functions which specify the probability for heavy quarks and gluons to hadronize into quarkonium bound states starting from perturbative QCD. These functions involve nonperturbative matrix elements whose values must still be extracted from experiment or the lattice. But their dependence upon the quarkonium longitudinal momentum fraction z can be calculated to lowest order in the strong interaction fine structure constant $\alpha_s(m_Q)$ and the velocity v of the heavy constituent quark inside the bound state. In principle, higher order corrections associated with these two small expansion parameters may be systematically evaluated as well. These developments have allowed a range of hadronization issues to be explored in a limited but model independent context.

The first fragmentation functions to be computed from perturbative QCD described the hadronization of gluons and heavy quarks into S-wave quarkonium bound states [1,2]. These $O(v^3)$ functions can be used to predict the direct production of η_c and J/Ψ charmonia as well as η_b and Υ bottomonia at lepton and hadron colliders. More recently, $O(v^5)$ P-wave fragmentation functions have also been calculated [3–5]. In this paper, we extend the ideas and methods developed in refs. [1–5] to the D-wave sector.

As $L = 2$ fragmentation functions start at $O(v^7)$, they are generally less important than those for $L = 0$ and $L = 1$ quarkonia. P-wave contributions to $Q \to \chi_Q$ have been found to be quite suppressed compared to S-wave terms [5], and D-wave effects should be even smaller still. On the other hand, gluon fragmentation to χ_Q is known to be phenomenologically significant at hadron machines where the number of gluons in the initial state is large. Indeed, the dominant source of high $p_\perp$ prompt J/Ψ's at the Tevatron is gluon fragmentation to χ_c's followed by single photon emission [6–8]. This prompt J/Ψ mechanism beats all others by almost two orders of magnitude. It is therefore interesting to examine the rate at which gluon fragmentation to D-wave quarkonia occurs as well.

We will focus in particular upon the production of the lowest lying charmonium state with the quantum numbers $n = 1$, $L = 2$ and $S = 0$. This $J^{PC} = 2^{-+}$ meson has not yet been observed. Quark model predictions for its mass fall within the range 3.81 GeV $\leq$ M $\leq$ 3.84 GeV which lies above the $D\overline{D}$ threshold [9–12]. But since its parity is odd, 1^1D_2 cannot decay to $D\overline{D}$, for the two spinless mesons would have to emerge in an even parity

1

$L = 2$ partial wave in order to conserve angular momentum. Moreover, the $n = 1$ state lies below the $D\overline{D}\pi$ and $D\overline{D}^*$ thresholds. Therefore, 1^1D_2 charmonium predominantly decays to lower $c\bar{c}$ levels or to light hadrons. Its width is consequently narrow. [1]

The wavefunction for a physical $^1D_2$ quarkonium can be decomposed into a series of Fock state components:

$$|^1D_2 \text{ Quarkonium}\rangle = |(Q\overline{Q})^{(1)}\rangle + O(v)|(Q\overline{Q})^{(8)}g\rangle + O(v^2)|(Q\overline{Q})^{(1,8)}gg\rangle + \cdots. \quad (1)$$

The superscript labels on the $Q\overline{Q}$ pairs indicate whether the heavy quark and antiquark reside within a color singlet or octet combination. The leading color singlet Fock component in (1) contributes to $g \to {}^1D_2$ fragmentation at $O(v^7)$ via the Feynman diagrams illustrated in fig. 1. These graphs mediate $^1D_2$ production through scattering processes like $gg \to gg^* \to gg\,{}^1D_2$. Such gluon fragmentation reactions dominate over lower order parton fusion processes when the energy q_0 of the incoming off-shell gluon g^* is large, but its squared four-momentum $s = q^2$ is close to the bound state's squared mass $M^2 \simeq (2m_Q)^2$. In this kinematic regime, the total cross section for $gg \to gg\,{}^1D_2$ factorizes up to $O(s/q_0^2)$ corrections which we neglect [1]:

$$\sigma(gg \to gg\,{}^1D_2) = 2 \times \sigma(gg \to gg) \int_0^1 dz D_{g\to {}^1D_2}(z). \quad (2)$$

The integrated fragmentation probability is thus simply given by the cross section ratio

$$\int_0^1 dz D_{g\to {}^1D_2}(z) = \frac{\sigma(gg \to gg\,{}^1D_2)}{2\sigma(gg \to gg)} = \frac{1}{16\pi^2} \int_{M^2}^{\infty} \frac{ds}{s^2} \int_0^1 dz\,\theta\Big(s - \frac{M^2}{z}\Big) \sum |A(g^* \to {}^1D_2 g)|^2. \quad (3)$$

Higher $^1D_2$ Fock state components also participate at $O(v^7)$ in $g \to {}^1D_2$ fragmentation. For example, the S-wave $(Q\overline{Q})^{(1,8)}$ pair inside the $|(Q\overline{Q})^{(1,8)}gg\rangle$ Fock state in eqn. (1) can be formed through the hard process $g^* \to {}^1S_0^{(1,8)}g$ as pictured in fig. 2. It subsequently converts to a physical $^1D_2$ quarkonium through the spin-preserving emission of two soft gluons. The short distance formation of the $^1S_0^{(1,8)}$ bound state takes place at $O(v^3)$ while the long distance gluon emissions each cost an additional power of v in the amplitude [15]. The graph in fig. 2 is therefore formally of the same order in the heavy quark velocity expansion as the diagrams in fig. 1.

---

[1] Nonrelativistic potential models yield the estimate $\Gamma \simeq 0.34$ MeV for the total width of the 1^1D_2 charmonium state [13,14].

Unfortunately, we do not know any rigorous way to determine the nonperturbative matrix elements associated with the higher $^1D_2$ Fock state components. However, previous experience with gluon and heavy quark fragmentation to P-wave quarkonia provides some guidance. In $g \to \chi_Q$ fragmentation, the $O(v^5)$ contribution from the color-octet term in the χ_Q wavefunction

$$|^3P_{0,1,2} \text{ Quarkonium}\rangle = |(Q\overline{Q})^{(1)}\rangle + O(v)|(Q\overline{Q})^{(8)}g\rangle + \cdots \tag{4}$$

contains one less power of the short distance fine structure constant $\alpha_s(m_Q)$ than the $O(v^5)$ color-singlet term and is numerically more important [3]. On the other hand, the color-singlet term is much larger than its color-octet counterpart in $Q \to \chi_Q$ fragmentation where both are $O\big(\alpha_s(m_Q)^2\big)$ [5]. Since the D-wave diagrams in figs. 1 and 2 are also of the same order in $\alpha_s(m_Q)$, the P-wave examples suggest it is reasonable to assume that the latter graph is numerically small. We will therefore simply neglect it in our analysis.

We proceed to evaluate the two diagrams displayed in fig. 1 by extending the Feynman rules for S and P-wave quarkonium processes derived in ref. [16] to D-wave bound states. Their sum yields the manifestly gauge invariant amplitude

$$iA\big(g_a^*(q) \to {}^1D_2(p) + g_b(p')\big) = -8\sqrt{\frac{15}{2\pi N_c M}}\frac{g_s^2\delta_{ab}}{(s-M^2)^3}R_2''(0)\varepsilon_\mu(q)\varepsilon_\nu(p')^*\varepsilon_{\alpha\beta}^{(h)}(p)^* $$
$$\times \, \epsilon^{\mu\nu\sigma\tau}q_\sigma p'_\tau(q+p')^\alpha(q+p')^\beta. \tag{5}$$

Here $N_c = 3$ denotes the number of colors, g_s represents the strong interaction coupling and $R_2''(0)$ equals the second derivative of the bound state's radial wavefunction evaluated at the origin. [2] Summing over the final gluon's color and polarization, we obtain the squared amplitude

$$\frac{1}{16\pi^2}\sum|A\big(g^*(q) \to {}^1D_2(p) + g(p')\big)|^2 = -\frac{1920\alpha_s^2}{\pi N_c}|R_2''(0)|^2\frac{(s-M^2)^2 g^{\mu\nu} + 4sp^\mu p^\nu}{M(s-M^2)^6}$$
$$\times\, q^\alpha q^\beta q^\gamma q^\delta \sum\varepsilon_\mu(q)\varepsilon_\nu(q)^* \sum\varepsilon_{\alpha\beta}^{(h)}(p)\varepsilon_{\gamma\delta}^{(h)}(p)^*. \tag{7}$$

---

[2] The $^1D_2$'s polarization tensor is related to its nonrelativistic wavefunction by

$$\int\frac{d^3\ell}{(2\pi)^3}\ell_\alpha\ell_\beta\psi_{2h}(\ell;p) = \sqrt{\frac{15}{8\pi}}\varepsilon_{\alpha\beta}^{(h)}(p)R_2''(0) \tag{6}$$

where ℓ_α represents the relative four-momentum between the heavy quark and antiquark inside the bound state. The polarization tensor's label h ranges over the helicity levels of the $J = 2$ meson.

3

The remaining spin sums for the individual helicity levels of the $J = 2$ quarkonium may be evaluated using the covariant expressions given in ref. [17]. To the order at which we are working, we can also set $p^\mu = zq^\mu + p_\perp$ and substitute $p^\mu p^\nu \to -\frac{1}{2}(1-z)(zs - M^2)g^{\mu\nu}$ [1]. Then after removing the factor $-g^{\mu\nu} \sum \varepsilon_\mu(q)\varepsilon_\nu(q)^*$ from eqn. (7), inserting the squared amplitude into eqn. (3), and swapping the order of the s and z integrations, we simply read off the polarized gluon fragmentation functions

$$
\begin{aligned}
D_{g \to {}^1D_2{}^{(h=0)}}(z, M) = {} & \frac{16\alpha_s(M)^2}{\pi N_c} \frac{|R_2''(0)|^2}{M^7} \Big[1080z^{-3} - 2340z^{-2} + 1680z^{-1} - 450 + 37z - 2z^2 \\
& + \left(1080z^{-4} - 2880z^{-3} + 2760z^{-2} - 1140z^{-1} + 190 - 10z \right) \log(1 - z) \Big]
\end{aligned}
$$

$$
\begin{aligned}
D_{g \to {}^1D_2{}^{(|h|=1)}}(z, M) = {} & \frac{64\alpha_s(M)^2}{\pi N_c} \frac{|R_2''(0)|^2}{M^7} (1 - z)\Big[-360z^{-3} + 420z^{-2} - 120z^{-1} + 5 + z \\
& + \left(-360z^{-4} + 600z^{-3} - 300z^{-2} + 45z^{-1} \right) \log(1 - z) \Big]
\end{aligned}
$$

$$
\begin{aligned}
D_{g \to {}^1D_2{}^{(|h|=2)}}(z, M) = {} & \frac{32\alpha_s(M)^2}{\pi N_c} \frac{|R_2''(0)|^2}{M^7} (1 - z)\Big[180z^{-3} - 210z^{-2} + 30z^{-1} + 5 + 2z \\
& + \left(180z^{-4} - 300z^{-3} + 120z^{-2} \right) \log(1 - z) \Big] \tag{8a}
\end{aligned}
$$

and their unpolarized sum

$$
D_{g \to {}^1D_2}(z, M) = \frac{80\alpha_s(M)^2}{\pi N_c} \frac{|R_2''(0)|^2}{M^7} \Big[3z - 2z^2 + 2(1 - z)\log(1 - z) \Big]. \tag{8b}
$$

The z dependence of this last expression is precisely the same as that of the $g \to \eta_c$ fragmentation function found in ref. [1].

The functions in eqns. (8a) and (8b) are evaluated at the renormalization scale $\mu = M$ which corresponds to the minimum allowed value for the fragmenting gluon's $\sqrt{s}$. They may be evolved to higher energies using the Altarelli-Parisi equation

$$
\mu \frac{dD_{g \to {}^1D_2}}{d\mu}(z, \mu) = \frac{\alpha_s(\mu)}{2\pi} \int_z^1 \frac{dy}{y} P_{gg}(y) D_{g \to {}^1D_2}\left(\frac{z}{y}, \mu\right) \tag{9}
$$

where

$$
P_{gg}(y) = 6\left[\frac{y}{(1 - y)_+} + \frac{1 - y}{y} + y(1 - y) + \frac{33 - 2n_f}{36}\delta(1 - y) \right] \tag{10}
$$

denotes the gluon splitting function for n_f active quark flavors. The $|h| = 0, 1$ and 2 polarized fragmentation functions for the lowest lying $n = 1$ ${}^1D_2$ charmonium state as well as their unpolarized sum are plotted in figs. 3a and 3b for $\mu = M$ and $\mu = 10M$ respectively. The results displayed in the figure are based upon the parameter values

4

$M = 3.82$ GeV, $\alpha_s(M) = 0.256$ and $|R_2''(0)|^2 = 0.07$ GeV^7 [13]. Comparing the low and high energy curves, we see that the weights of all the fragmentation functions are shifted toward lower values of z as the renormalization scale increases. This behavior is consistent with the general effect of Altarelli-Parisi running upon any fragmentation function.

An approximate estimate for the rate of prompt $^1D_2$ quarkonia production at hadron colliders is given by the product of the total cross section for gluon production and the initial integrated fragmentation probability

$$D_{g \to {}^1D_2}(M) = \frac{80\alpha_s^2(M)}{3\pi N_c} \frac{|R_2''(0)|^2}{M^7}. \tag{11}$$

In the particular case of 1^1D_2 charmonium, we find $D_{g \to 1^1D_2}(M) \simeq 1.0 \times 10^{-6}$. It is instructive to compare this D-wave fragmentation probability with the corresponding S-wave result [1]

$$D_{g \to \eta_c}(M_{\eta_c}) = \frac{\alpha_s^2(M_{\eta_c})}{3\pi N_c} \frac{|R_0(0)|^2}{M_{\eta_c}^3} \simeq 5.3 \times 10^{-5} \tag{12}$$

where $M_{\eta_c} = 2.98$ GeV, $\alpha_s(M_{\eta_c}) = 0.282$ and $|R_0(0)|^2 = 0.5$ GeV^3. Although the rate for $g \to 1^1D_2$ is formally suppressed by four powers of v compared to that for $g \to \eta_c$, the probability of the former is enhanced by a numerical prefactor of 80 relative to the latter. Gluon fragmentation to the D-wave bound state is therefore larger than one might have initially anticipated.

A more precise prediction for $^1D_2$ production may be obtained by folding together the Altarelli-Parisi evolved fragmentation functions and the gluon cross section $d\sigma(p\bar{p} \to g + X)/dp_\perp$ into the combination

$$\frac{d\sigma(p\bar{p} \to {}^1D_2{}^{(h)} + X)}{dp_\perp} = \int_0^1 dz \frac{d\sigma(p\bar{p} \to g(p_\perp/z) + X, \mu)}{dp_\perp} D_{g \to {}^1D_2{}^{(h)}}(z, \mu). \tag{13}$$

This transverse momentum distribution is displayed in fig. 4 for 1^1D_2 charmonium production in the pseudorapidity range $|\eta| \leq 0.6$ at the Tevatron. We have used the MRSD0 parton distribution function evaluated at $\mu = M_\perp/z = \sqrt{M^2 + p_\perp^2}/z$ to generate the differential cross section shown in the figure.

Since the gluon cross section is a steeply falling function of $p_\perp$, the main support for the integral in eqn. (13) lies near $z = 1$. Looking again at the fragmentation functions in figs. 3a and 3b, we see that the $h = 0$ helicity component dominates over the other helicity levels for z close to unity. As a result, the $h = 0$ differential cross section in fig. 4 is

larger than its $|h| = 1$ and $|h| = 2$ counterparts. Over the transverse momentum interval $5 \text{ GeV} \le \text{p}_\perp \le 30 \text{ GeV}$, the ratio of these cross sections is approximately given by

$$\frac{d\sigma^{(h=0)}}{dp_\perp} : \frac{d\sigma^{(|h|=1)}}{dp_\perp} : \frac{d\sigma^{(|h|=2)}}{dp_\perp} \simeq 1.00 : 0.79 : 0.34. \tag{14}$$

Recall that the helicity levels for an unpolarized $J = 2$ state would be populated according to

$$\frac{d\sigma^{(h=0)}}{dp_\perp} : \frac{d\sigma^{(|h|=1)}}{dp_\perp} : \frac{d\sigma^{(|h|=2)}}{dp_\perp} \simeq 1 : 2 : 2. \tag{15}$$

Gluon fragmentation consequently induces a sizable $^1D_2$ alignment. This polarization can be observed in the angular distribution of photons

$$\frac{d\Gamma}{d\cos\theta} \propto 1 - 0.33\cos^2\theta \tag{16}$$

which result from the dominant E1 radiative transition $1^1D_2 \rightarrow 1^1P_1 + \gamma$ [17]. A measurement of this angular distribution would provide a test of the $g \rightarrow {}^1D_2$ fragmentation picture.

The integral of $d\sigma(p\overline{p} \rightarrow 1^1D_2 + X)/dp_\perp$ over the transverse momentum range $p_\perp \ge M$ where the results of our gluon fragmentation calculation can be trusted yields 0.8 nb. We should stress that this integrated Tevatron cross section value represents a conservative lower bound. Higher Fock state contributions to $g \rightarrow 1^1D_2$, charm quark fragmentation and parton fusion processes will all enhance the production of 1^1D_2 charmonia. The D-wave state should therefore be produced at a nonnegligible rate.

Detecting $J^{PC} = 2^{-+}$ charmonia will not be simple however. One decay mode which might be observable is $1^1D_2 \rightarrow \psi' + \gamma$. This M1 radiative transition connects the $^1D_2$ initial state to the $^3D_1$ component of the physical ψ' [18]. It is suppressed by the small mixing angle which accompanies the $L = 2$ component. Another possible mode which may be experimentally feasible to reconstruct is the following:

1. $1^1D_2 \rightarrow 1^1P_1 + \gamma$ Br $\simeq 0.80$ [13, 14]

2. $1^1P_1 \rightarrow J/\Psi + \pi^0$ Br $\simeq 0.005$ [19]

3. $J/\Psi \rightarrow \mu^+\mu^-$ Br $\simeq 0.06$ [20].

Approximate branching ratios for the steps in this decay chain are listed on the right. In order to overcome the small value for their product, a data sample corresponding to a

large integrated luminosity will have to be collected. The 1^1D_2 event rate may then be high enough to detect in this channel.

In conclusion, we have investigated gluon fragmentation to heavy $^1D_2$ quarkonia in perturbative QCD. We have found that the polarized $g \to {}^1D_2$ fragmentation functions are enhanced by large numerical prefactors and yield $J^{PC} = 2^{-+}$ mesons which are significantly aligned. These results provide motivation to search for these D-wave states in the future.

Figure Captions

Fig. 1.   Lowest order color-singlet Feynman diagrams which mediate $g \to {}^1D_2$ fragmentation.

Fig. 2.   An example of a higher order Fock component contribution to $g \to {}^1D_2$ fragmentation. The ${}^1S_0^{(1,8)}$ bound state which is formed at short distances emits two soft gluons to become a physical ${}^1D_2$ quarkonium.

Fig. 3. $g \to 1{}^1D_2$ charmonium fragmentation functions evaluated at (a) $\mu = M$ and (b) $\mu = 10M$. The dotted, dot-dashed and dashed curves represent the fragmentation functions for the $|h| = 0$, 1 and 2 helicity components of the $J = 2$ bound state, while the solid curve illustrates their sum.

Fig. 4.   Transverse momentum differential cross section for $1{}^1D_2$ charmonium production at the Tevatron. The dotted, dot-dashed and dashed curves represent the cross sections for the $|h| = 0$, 1 and 2 helicity components of the $J = 2$ bound state, while the solid curve illustrates their sum.

References

[1] E. Braaten and T.C. Yuan, Phys. Rev. Lett. **71** (1993) 1673.

[2] E. Braaten, K. Cheung and T.C. Yuan, Phys. Rev. **D48** (1993) 4230.

[3] E. Braaten and T.C. Yuan, Phys. Rev. **D50** (1994) 3295.

[4] Y.-Q. Chen, Phys. Rev. **D48** (1993) 5181.

[5] T.C. Yuan, UCD-94-2 (1994) unpublished.

[6] E. Braaten, M. A. Doncheski, S. Fleming and M. L. Mangano, Fermilab-pub-94/135-T (1994), unpublished.

[7] M. Cacciari and M. Greco, FNT/T-94/13 (1994), unpublished.

[8] D.P. Roy and K. Sridhar, CERN-TH.7329/94 (1994), unpublished.

[9] E. Eichten and F. Feinberg, Phys. Rev. **D23** (1981) 2724.

[10] W. Buchmüller, Phys. Lett. **B112** (1982) 479.

[11] S. Godfrey and N. Isgur, Phys. Rev. **D32** (1985) 189.

[12] W. Kwong, J.L. Rosner and C. Quigg, Ann. Rev. Nucl. and Part. Sci., **37** (1987) 325.

[13] V.A. Novikov, L.B. Okun, M.A. Shifman, A.I. Vainshtein, M.B. Voloshin and V.I. Zakharov, Phys. Rept. **41C** (1978) 1.

[14] E. Eichten, K. Gottfried, T. Kinoshita, K.D. Lane and T.-M. Yan, Phys. Rev. **D17** (1978) 48.

[15] G.T. Bodwin, E. Braaten and G.P. Lepage, ANL-HEP-PR-94-24 (1994) unpublished.

[16] J. H. Kühn, J. Kaplan and E. G. O. Safiani, Nucl. Phys. **B157** (1979) 125;
B. Guberina, J.H. Kühn, R.D. Peccei and R. Rückl, Nucl. Phys. **B174** (1980) 317.

[17] P. Cho, S. Trivedi and M. Wise, CALT-68-1943 (1994), unpublished.

[18] F.E. Close, RAL-94-093 (1994), unpublished.

[19] Y.-P. Kuang, S.F. Tuan and T.-M. Yan, Phys. Rev. **D37** (1988) 1210.

[20] Review of Particle Properties, Phys. Rev. **D50**, Part I (1994).

This figure "fig1-1.png" is available in "png" format from:

http://arXiv.org/ps/hep-ph/9410214v1

This figure "fig1-2.png" is available in "png" format from:

http://arXiv.org/ps/hep-ph/9410214v1
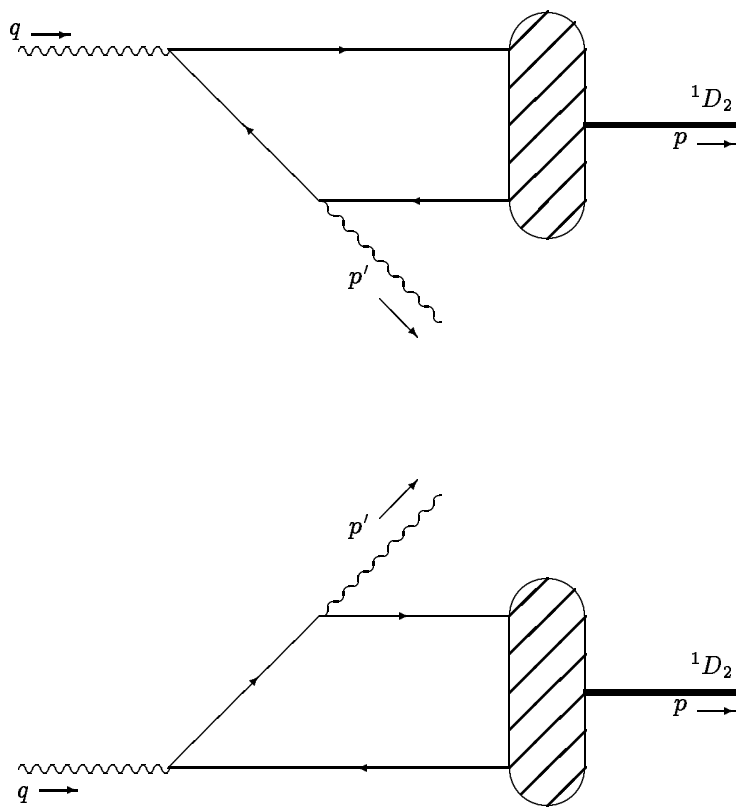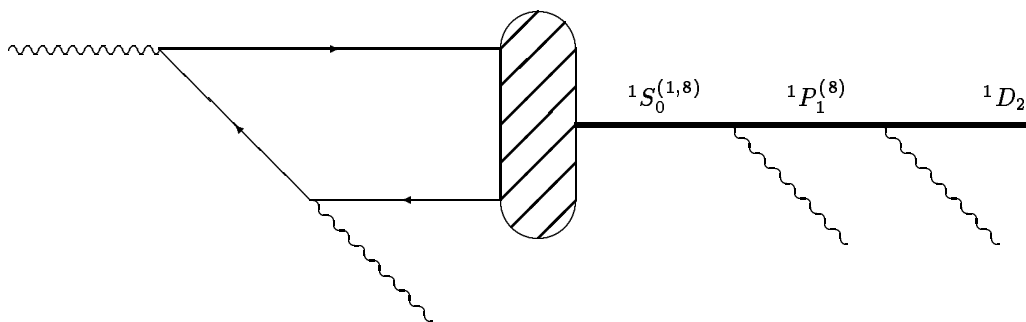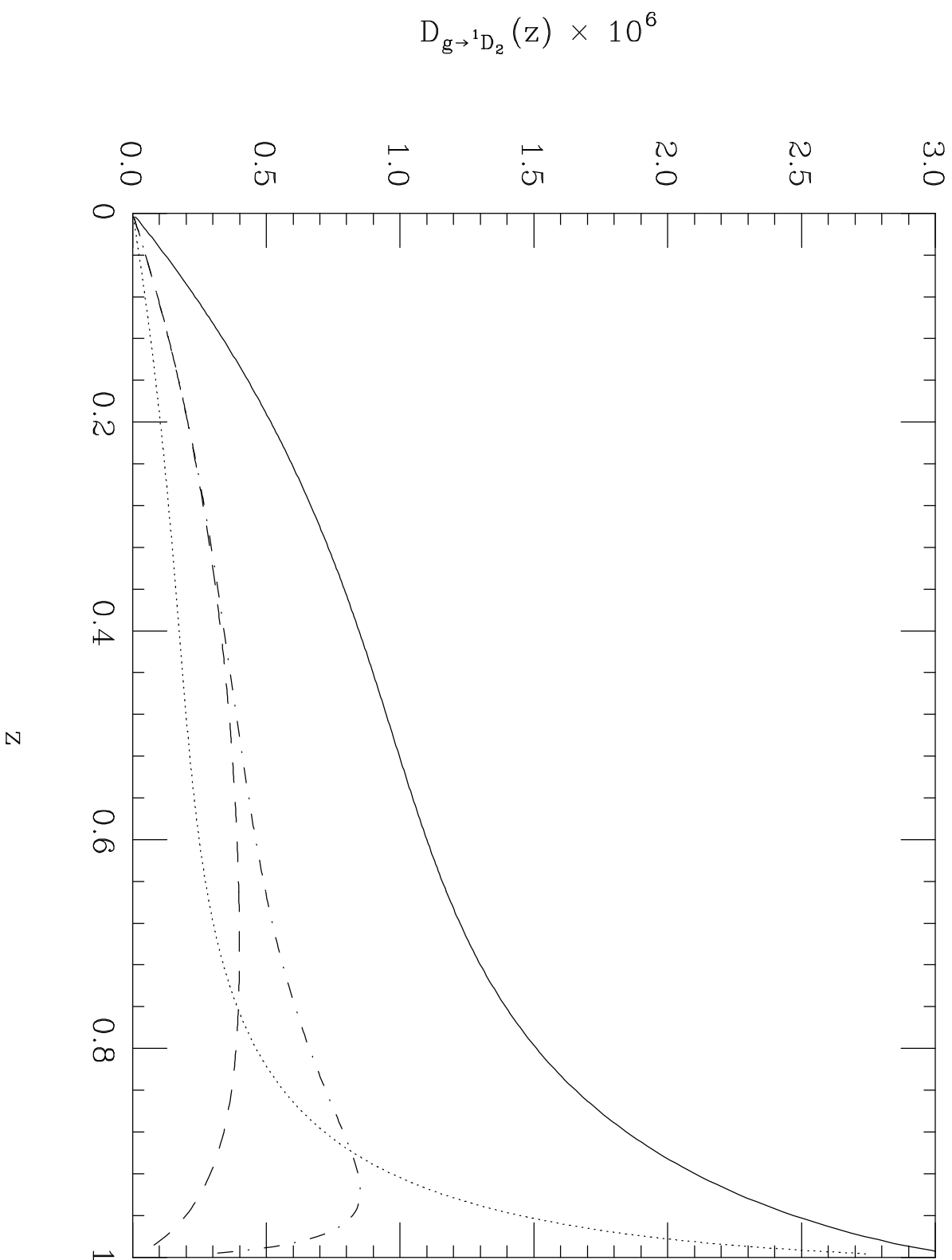
Figure 1

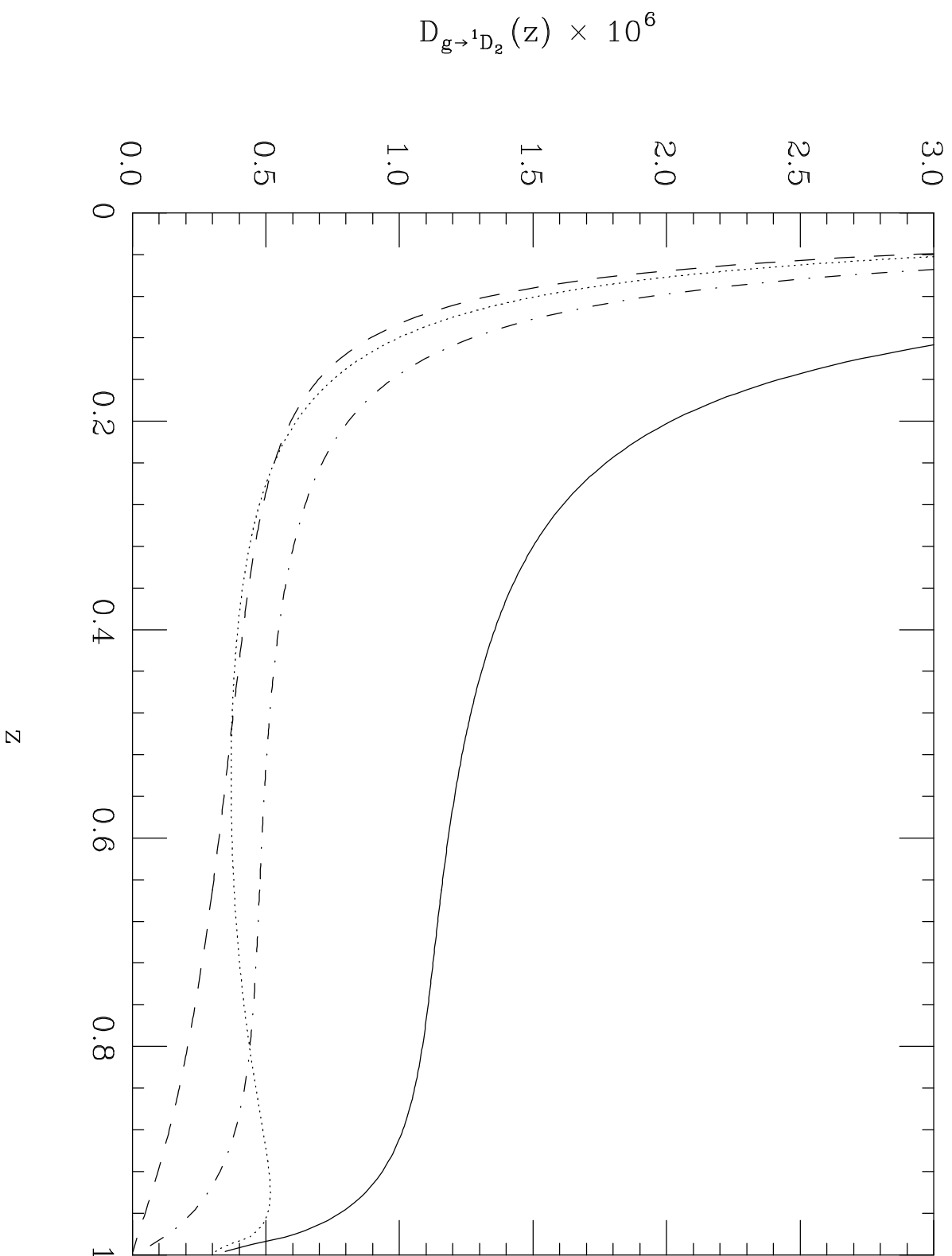Figure 2

This figure "fig1-3.png" is available in "png" format from:

http://arXiv.org/ps/hep-ph/9410214v1

Figure 3a

$D_{g \rightarrow {}^1D_2}(z) \times 10^6$

z

Figure 3b

This figure "fig1-4.png" is available in "png" format from:

http://arXiv.org/ps/hep-ph/9410214v1

$d\sigma(P\overline{P} \rightarrow {}^1D_2+X)/dp_\perp$ (nb/GeV)

$p_\perp$ (GeV)

Figure 4